Available online at www.eccomasproceedia.org
Eccomas Proceedia COMPDYN (2017) 975-989

ECCOMAS
Proceedia

COMPDYN 2017
6th ECCOMAS Thematic Conference on
Computational Methods in Structural Dynamics and Earthquake Engineering
M. Papadrakakis, M. Fragiadakis (eds.)
Rhodes Island, Greece, 15–17 June 2017

EFFECT OF GROUND MOTION DIRECTIONALITY ON SEISMIC RESPONSE OF BASE-ISOLATED BUILDINGS CONSIDERING POUNDINGS TO ADJACENT STRUCTURES

Eftychia A. Mavronicola[1] and Petros Komodromos[2]

Department of Civil and Environmental Engineering, University of Cyprus
75 Kallipoleos Street, P.O.Box 20537, 1678 Nicosia, Cyprus

[1]mavronicola.eftychia@ucy.ac.cy, [2]komodromos@ucy.ac.cy

Keywords: ground motion directionality, structural impacts, base-isolated building, adjacent structures.

Abstract. *Base isolation has proven an effective strategy to minimize structural and non-structural damage, prevent functionality disruption and protect sensitive equipment in buildings even under strong ground motions. However, structural pounding with the surrounding moat wall and/or adjacent buildings may induce local and even severe damages to base-isolated structures. This study utilizes a computational methodology that enables the investigation of poundings in a three-dimensional (3D) domain, while considering the arbitrary location of contact points and the geometry at the vicinity of impact; it aims to investigate the circumstances under which spatial pounding may occur and quantify their effect on the response of the base-isolated structure. Given that the seismic response of base-isolated structures subjected to strong ground motions depends on the excitation characteristics, namely frequency content and horizontal ground motion directionality, the sensitivity of the calculated nonlinear dynamic response of a 3-story base-isolated building during pounding against other fixed-supported buildings is thoroughly and parametrically examined. Numerous nonlinear time history analyses are performed on the structural model using selected pairs of recorded horizontal ground-motion orthogonal components. Records are rotated to 73 different horizontal angles of incidence with respect to the building's structural axes in the range of 0 to 360 degrees. The influence of different parameters, such as the type and the location of the adjacent-fixed supported buildings, is also investigated. The significant influences of (a) the excitation angle and (b) the structural configuration arrangement on the overall peak seismic response are highlighted and quantified.*

doi: 10.7712/120117.5470.17252

1 INTRODUCTION

The incorporation of significant lateral flexibility at the isolation level is commonly employed as a seismic isolation strategy to improve the seismic performance of a structure. Subsequently, the introduced flexibility is expected to result in large relative displacements at the isolation level during a strong earthquake excitation. In order to accommodate these expected large deformations, a wide seismic gap should be provided, as a clearance, around the building. This requirement imposes a practical constraint for the utilization of seismic isolation, considering that there are often certain practical restrictions to the size of the available clearances around seismically isolated buildings, especially in cases of retrofitting of existing buildings in densely resided civic centers. Since the width of the available clearance is often limited, a reasonable concern is the risk of structural pounding with the surrounding moat wall or adjacent structures during very strong earthquakes.

Although, the problem of earthquake-induced pounding has been the subject of great scientific interest, very limited research work has been carried out for poundings of seismically isolated buildings. The majority of those research works simulate the problem in two-dimensions [1–9], in an attempt to avoid the complexities associated with the 3D nature of the problem and the consequently excessive computational cost. However, the effect of crucial factors, which may excite the torsional vibration of a building and further increase the possibility of impacts during earthquakes, can be taken into consideration only through 3D simulations.

A number of recent research works that extend the simulation in the more realistic 3D space [10–19] have been reported. Matsagar and Jangid [10] investigated the seismic response of a single-story asymmetric structure supported on various base-isolation systems during impact with adjacent structures. Jankowski [11,12] simulated, using a commercially available software, a case of pounding between the Olive View Hospital main building and one of its independently standing stairway towers during the San Fernando earthquake of 1971. In that work, a detailed 3D pounding-involved response analysis of two adjacent structures had been conducted using the finite element method with a non-linear model of material behavior, including stiffness degradation of concrete under cyclic loading. Uz and Hadi [13] carried out a parametric investigation of pounding involved response of two base-isolated buildings of unequal heights. Nonlinear analysis had been used, modeling the structures with inelastic MDOF lumped mass systems. The nonlinear viscoelastic model to assess the proper impact force during collisions had been incorporated on the 3D pounding between two adjacent four- and three-story buildings. The effects of seismic pounding on the structural performance of a base-isolated reinforced concrete building were investigated by Pant and Wijeyewickrema [15,16], aiming to evaluate the influence of adjacent structures and the separation between structures on the pounding response. Specifically, 3D finite element analyses of the base-isolated building were carried out considering various seismic excitations.

While 3D simulations of structures impacting with neighboring buildings have already been reported in the scientific literature, a systematic parametric investigation of the controlling properties on the overall seismic response is still lacking. In this paper, selected results for spatial numerical simulations and parametric studies of a 3-story base-isolated building that may collide with the surrounding moat wall and/or adjacent conventionally fixed-supported buildings during strong earthquake excitations are presented. Nonlinear time-history analyses are carried out considering the arbitrary direction of selected bidirectional ground-motions with respect to the structural axes of the simulated structures. The influence of the separation distance between the adjacent structures is also investigated, while considering different geometrical arrangements for the surrounding structures.

2 SPATIAL (3D) SIMULATION METHODOLOGY

This research work utilizes the computational methodology described in [18,20], aiming to thoroughly investigate the circumstances under which spatial pounding of base-isolated buildings may occur and assess the effect of some important parameters on the peak structural response due to potential structural pounding. In order to efficiently and effectively estimate the impact forces that should be applied at detected impact points on each structure in contact, an appropriate 3D impact model is used. More precisely, a "penalty" method has been implemented [20], in which a small interpenetration among two colliding bodies is allowed and used in combination with an impact stiffness coefficient to calculate the elastic impact forces that should be applied on the colliding bodies. It should be mentioned that in the methodology used herein, the area of the overlapping region, instead of the interpenetration depth, is used as the key variable in the calculation of impact forces. Figure 1 shows how the proposed impact model works.

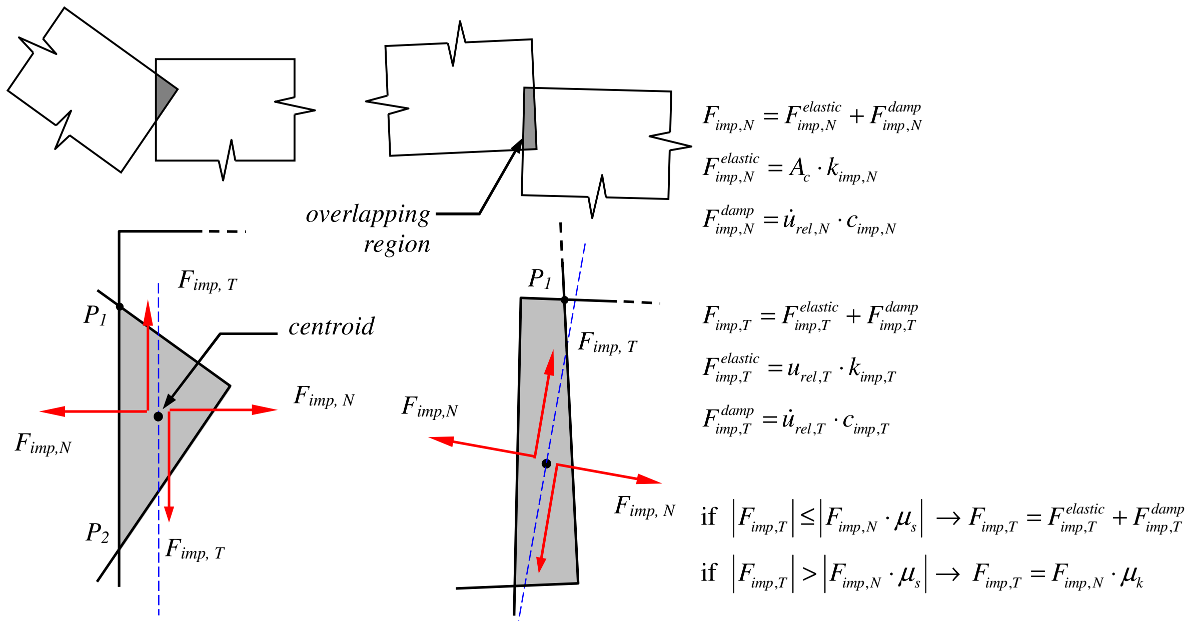

Figure 1: Schematic representation of the contact plane based on the geometry of the indentation region, which can be either a triangle, or a quadrilateral.

In particular, when two bodies come in contact, they form an overlapping region that is either a triangle or a quadrilateral. The algorithm uses the geometry of the overlapping region at each time-step, defined by the coordinates of its nodes, in order to determine: (i) the location of the action point of the impact forces, (ii) the direction of the impact forces, based on the definition of the contact plane, and (iii) the magnitude of the impact forces. Contrary to the corresponding 2D impact models, the 3D impact model is able to calculate not only the normal impact forces, but also the frictional forces that may arise between the colliding structures. The Coulomb law of friction restricts the magnitude of the tangential impact force below or equal to a critical sliding value.

3 DATA ANALYSIS

A 3-story (three-bay by three-bay), base-isolated reinforced concrete moment-frame building is chosen as a typical model structure (Figure 2). The building is symmetric with coinciding centers of mass and stiffness. The retaining walls extend from the ground level up to the base level of the building. All column sections of the simulated building have square dimensions of 45 x 45 cm^2. The bay width of the building in both directions is 5.5 m while each story height is 3.2 m. The elastic modulus of concrete is assumed to be 30 GPa with a Poisson's ratio of 0.2. A uniformly distributed mass of 250 tons is considered for the roof mass, while a 340 tons floor mass is assumed at each other floor level, including the base of the building. For the determination of the Rayleigh damping matrix, the viscous damping ratios for the first and the fourth eigenfrequencies are taken as 0.05 and 0.02, respectively. Due to symmetry, the first two eigenmodes are translational along the two horizontal axes.

A coupled plasticity model is used for simulating the bidirectional lateral response of the seismic isolators. The aforementioned model is based on the hysteretic behavior proposed by Wen, 1976 [21] and Park *et al.*, 1986 [22] and recommended by Nagarajaiah *et al.*, 1991 [23]. Here, for each bearing element an isolation period based on the post-yield stiffness of 2.0 seconds, a yield displacement equal to 1.0 cm and a normalized characteristic strength F_{yi}/W_{tot} of 0.05, in both directions, are considered.

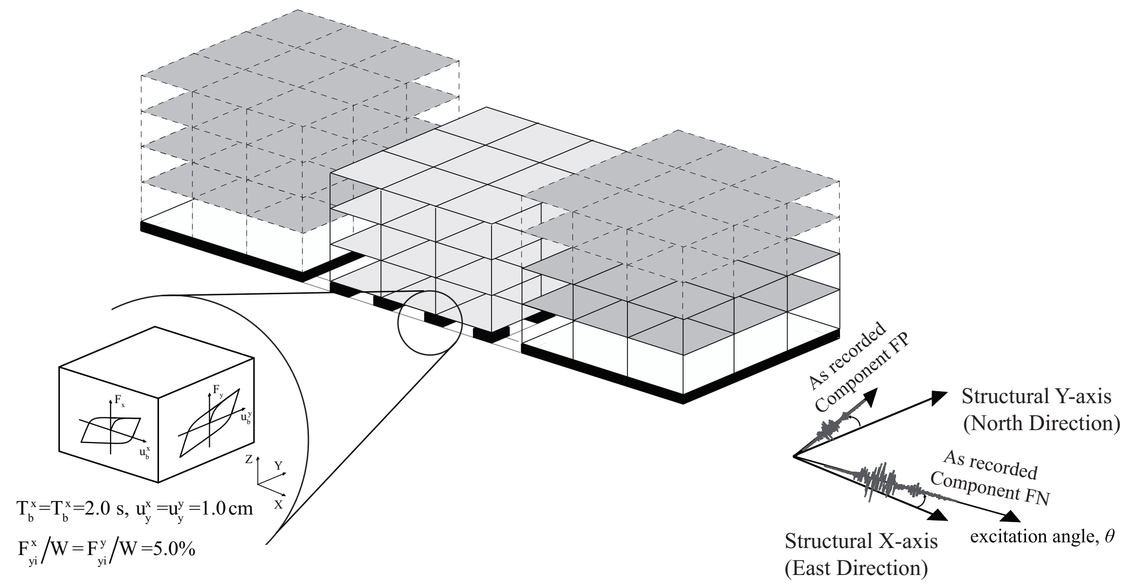

Figure 2: Schematic of a base-isolated building subjected to bidirectional excitation while surrounded by fixed-supported structures.

In the simulations performed within this paper, the 3-story seismically isolated building is considered to be adjacent to 2, 3, or 4-story fixed-supported buildings, which are located either on one or both sides of the base-isolated building, with the possibility of poundings occurring not only at its base with the moat wall but also at the upper floors of the buildings due to the deformation of their superstructures. The moat wall is modeled as a single-mass system, with three dynamic DOF, as in the case of a single-story structure. The moat wall is taken to be 100 cm thick and 100 cm high, resulting in a substantially stiff barrier, while it's mass is assumed to be 5 tons/m, a number that takes into consideration the contribution of the backfill soil. The normal impact stiffness is $k_{imp,N}$=2.58×10^7 KN/m^2, while the corresponding tangential impact stiffness is $k_{imp,T}$=5.74×10^6 KN/m. The static and kinetic friction coefficients are taken as μ_s=0.8 and μ_k=0.6, respectively. Surrounding buildings are simulated as linear MDOF systems, possessing the same superstructures' characteristics as the base-isolated building (except otherwise stated in the text) and located in the same distance as the adjacent moat wall. For simplicity, it is assumed that the floor-slabs of the neighboring buildings are located at the same levels, leading to potential slab-to-slab poundings and neglecting any slab-to-column interactions. In cases when adjacent structures are located on both sides of the base-isolated building, the separation gap is considered to be the same.

A set of earthquake ground motions, rotated to fault-normal (FN) and fault-parallel (FP) components, has been selected from the Pacific Earthquake Engineering Research Center database. The selected seismic accelerograms (Table 1) are expected to induce large relative displacements to the seismically isolated building, since they are characterized by low-frequency contents, which is one of the most decisive factors for the occurrence of pounding in such structures.

NGA#	Event	Year	Station	M_w	Comp	PGA (g)	PGV (cm/s)	PGD (cm)
779	Loma Prieta	1989	LGPC	6.93	FN	0.94	97	62.5
					FP	0.54	72.1	30.5
821	Erzican- Turkey	1992	Erzincan	6.69	FN	0.49	95.4	32.1
					FP	0.42	45.3	16.5
1045	Northridge-01	1994	Newhall -W Pico Canyon Rd.	6.69	FN	0.43	87.7	55.1
					FP	0.28	74.7	21.8
1084	Northridge-01	1994	Sylmar – Converter Sta	6.69	FN	0.59	130.3	54
					FP	0.8	93.3	53.3
2114	Denali- Alaska	1999	TAPS Pump Station #10	6.2	FN	0.33	95.5	92.4
					FP	0.27	121.3	116.2

Table 1: Summary of the main characteristics of the selected horizontal seismic excitations.

4 PARAMETRIC ANALYSIS RESULTS

4.1 Effect of Seismic Orientation on the Peak Response without pounding

Before proceeding with the investigation of structural poundings, a series of simulations on the individual dynamic response of the base-isolated and fixed-supported buildings considered herein is undertaken. The peak unobstructed relative displacements of the buildings in the X-direction are illustrated in Figure 3. The structures are analyzed for the 5 bidirectional ground-motions, each one rotated with a constant step of 5° in the range of 0° to 360°. The main results arising from these simulations with regards to the ground motion orientation effect, are in line with previous observations [18] (i) the incidence angle of excitation significantly affects the maximum response of the structures in the X-direction, (ii) the critical angle corresponding to the peak response over all possible excitation orientations varies with the selected ground motion and the dynamic characteristics of the structures, and (iii) the FN/FP drifts (θ=0°) are not always conservative.

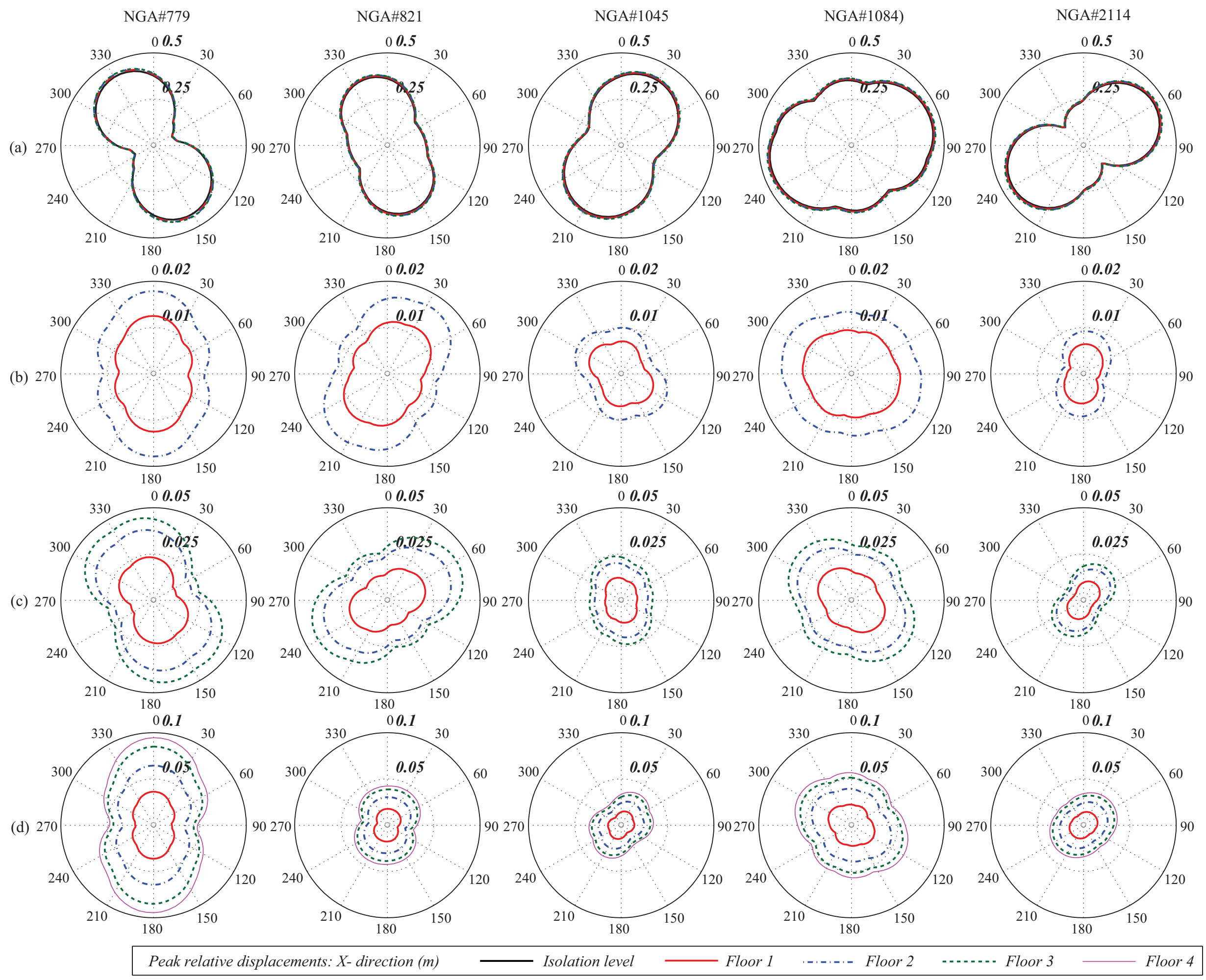

Figure 3: Peak unobstructed relative displacements of (a) the 3–story base-isolated building, and (b) the 2–story, (c) 3–story, and the (d) 4–story; fixed–based structures, in X-direction, in terms of the incidence angle.

4.2 Effect of Adjacent Structural Arrangement

Given that the seismic response of base-isolated structures subjected to strong excitations depends on the excitation characteristics, specifically the frequency content and horizontal ground-motion directionality, the sensitivity of the calculated nonlinear dynamic response of a 3-story seismically isolated building during pounding against other fixed-supported buildings and/or the surrounding wall is parametrically examined. Numerous nonlinear time-history analyses are performed using selected pairs of recorded horizontal ground-motion orthogonal components.

The peak responses of the examined seismically isolated building are discussed next, assuming an available seismic gap between the simulated structure and the adjacent structures of 20 cm. Figure 4 presents the peak interstory drift ratios (resultant) at each floor of the base-isolated building among all corner columns during poundings with the adjacent structures, for all possible orientations of the ground motions. Records are rotated to 73 different horizontal angles of incidence with respect to the building's structural axes. It can be observed from Figure 4(a) that the peak interstory deflection ratios for the case of isolated building pounding against the surrounding moat wall occur at the isolation level, the 1-0 interface, and are in general higher than for the case of buildings in series, as given in Figure 4(b)-(d). Furthermore, the peak response of the base-isolated building decreases when moving from the ground floor upwards. This is in contrast to the response of buildings in series, which suggests that higher modes of deformation are activated in those cases; this observation is persistent for all earthquake excitations considered herein.

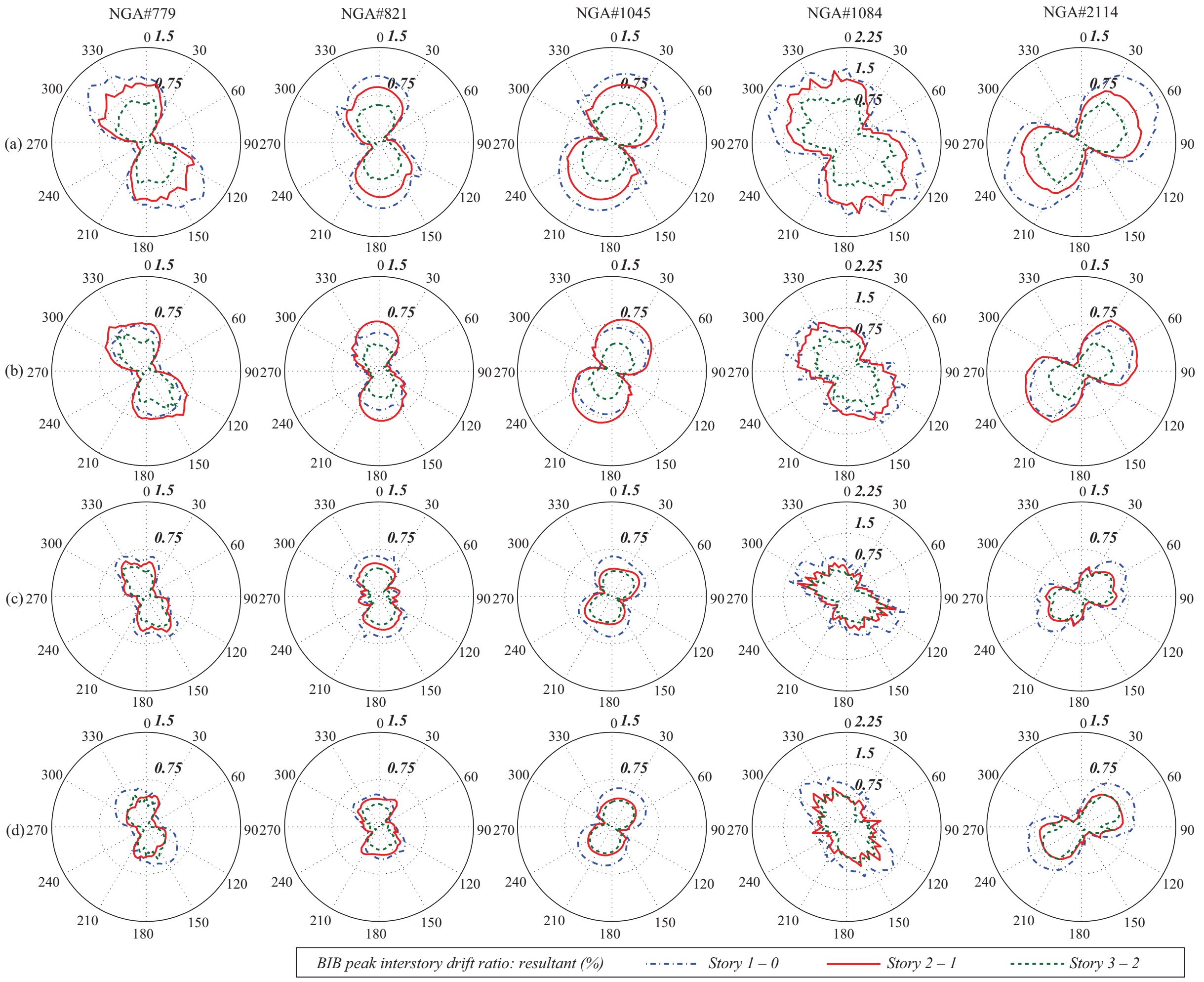

Figure 4: Peak responses of the 3-story base-isolated building among all corner columns in terms of the angle of incidence, during poundings with the (a) moat wall, and (b) 2-story, (c) 3-story (d) 4-story fixed-supported structures, located on both sides (west and east) of the seismically isolated building.

In the specific parametric analyses, the peak response ratios are located (i) at the isolation level, for the cases when only moat walls surround the building, and when the seismically isolated building is of equal height or shorter than the neighboring fixed-supported buildings, or (ii) at the same floor level as the roof of the adjacent fixed-base structures, which occurs when the adjacent structures are shorter than the base-isolated one, among all incidence angles of the excitations. In general, the polar plots suggest that the critical envelope for all excitation angles may not be dominated by the response of a specific floor but rather of the combination of the peak responses of several floors when the base-isolated building hits against the adjacent MDOF structures. In general, the effect of the ground motion directionality, in combination with the number of stories and, consequently, the fundamental eigenperiod of the adjacent structures seems to play a significant role to the severity of the structural response. It should be noted, however, that in the cases of buildings in series, the floor that dominates the critical envelope might change as the provided gap size is modified, which is further investigated below.

In order to assess the effect of specific structural arrangement (fixed-supported building on one side *vs.* both sides) on the overall dynamic response, a re-presentation of the results shown in Figure 4 is provided in Figure 5(a). More specifically, Figure 5 shows polar plots of the envelopes of peak interstory drift ratios during the five selected ground motions that are compared for six different configurations regarding: (i) the location of the adjacent fixed-supported buildings and (ii) the number of floors of the adjacent building (2, 3 or 4). In general, the variation of the response ratios, seems to be influenced by the earthquake excitation's characteristics (frequency content and directionality); as these plots show that peak interstory deflection ratios can vary by a factor of 2.5 over the possible angles of interest, at least for the gap size of 20 cm considered herein. It is interesting to note that, in general, the incidence angle at which the maximum amplification of the superstructure response due to pounding occurs coincides with the critical angle that corresponds to the peak relative displacement at the isolation level, as shown in Figure 3(a). We can also observe that when adjacent buildings are located on both sides of the base-isolated building, Figure 5(a), the polar plots of its peak responses for each floor exhibit 8-shape figures (a consequence of double symmetry), a characteristic that breaks down when a building is located only on one side, which leads to asymmetric response shapes as shown in Figure 5(b).

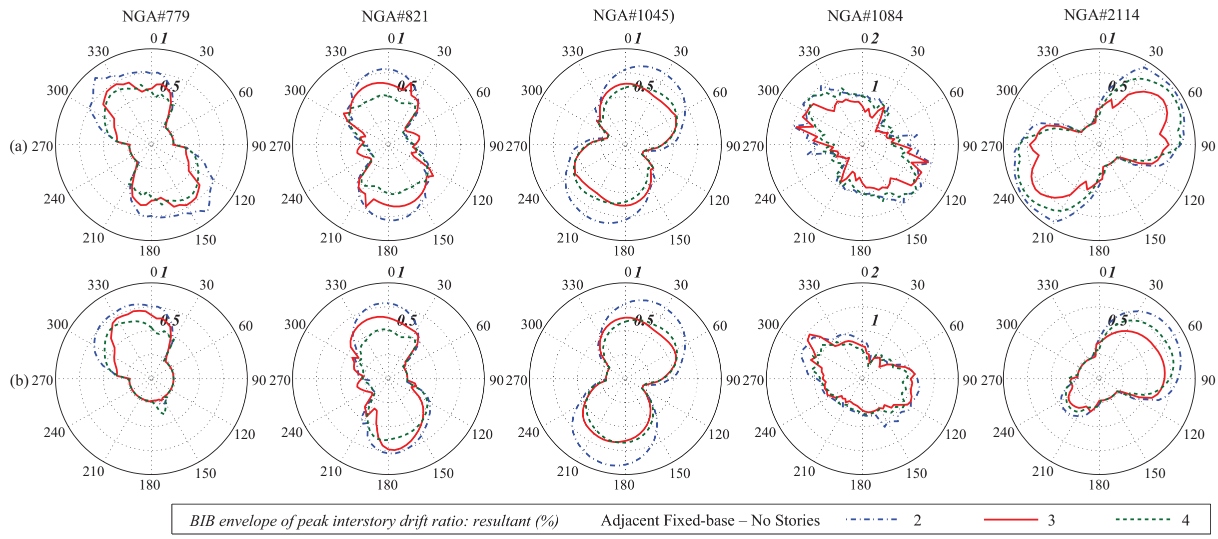

Figure 5: Envelope of peak resultant interstory drifts ratio of the seismically isolated building during poundings, in terms of the angle of incidence considering a gap size of 20 cm and various configurations of the adjacent fixed-supported structures, located (a) on both sides, (b) on the east side of the 3-story base-isolated structure.

Furthermore, the presence of fixed-supported buildings on both sides of the seismically isolated building has minor influences on the peak response during pounding for the ground motion critical orientation. For example, in the case of the Loma Prieta 1989 ground motion (NGA#779), the range of critical angles between 300° to 360°, and the envelope of the peak responses among all floors are relatively close irrespective of whether adjacent buildings are located on both sides or on a single (east) side. As anticipated, the location of the adjacent buildings, in combination with the excitations' characteristics affect the envelope of the peak response of the seismically isolated building during impact. Furthermore, Figure 5 suggests that the number of floors of the adjacent buildings can significantly affect the overall dynamic response of the base-isolated structure. Nevertheless, one cannot generalize the severity of the influence based on the number of floors. Results that are presented in the following sections, suggest that the number of floors by its own is not the only structural characteristic that defines the dynamic response of the base-isolated building. Other parameters such as stiffness, fundamental eigenperiod, etc. might shift the relative importance of having short *vs.* high buildings. What one can generalize is that the critical response is polarized at a specific direction irrespective of the number of stories of surrounding buildings. Considering that the critical angle varies significantly with the arrangement type, its estimation, without a detailed investigation, is difficult.

The incidence angle of the imposed seismic excitation seems to be an important factor while computing the peak seismic response of buildings. For design purposes, the evaluation of the critical conditions for each specific case, which could ensure the more reliable prediction of the peak structural response, is crucial. Therefore, it might be a mandate to perform 3D analysis and use an advanced modelling approach to determine the critical response for each case, with computational aid, where nonlinear analysis of the building at multiple angles of incidence should be considered.

4.3 Effect of Separation Distance

In order to investigate the influence of the gap size between adjacent structures, the base-isolated building is assumed to be separated by various distances from the adjacent structures. In Figure 6, the responses of the 3-story seismically isolated building are computed under four different configurations regarding the number of floors (2-, 3- and 4-floors) of the adjacent fixed-based structures located at both sides (east and west). The results for a single incidence angle (θ=0°) for five ground motions are presented. As anticipated, the location and the characteristics of the adjacent structures, in combination with the excitation characteristics affect the response of the seismically isolated structure during impact.

Figure 6 suggests that the peak interstory drift ratios of the base-isolated structure pounding with the moat wall are, in general, higher than those for the case of buildings in series. The fact that the base-isolated building pounds with the fixed-base building before it can impact the rigid retaining wall at the base, reduces the severity of impact at the base of the building for the range of separation distances examined. Furthermore, the ground floor of the base-isolated building dominates the peak response when only pounding with the surrounding wall at the base is considered. On the other hand, upper stories may experience higher drifts compared to lower level stories when pounding with adjacent fixed-base buildings is considered. More specifically, in the latter case the floor that dominates the critical envelope may change as the available gap size is modified. Also, it can be observed from Figure 6 that the critical gap size to avoid pounding, slightly increases in case of buildings in series. This is reasonable, considering that the seismically isolated building may pound against the neighboring buildings at the upper floors due to the deformations of the superstructures of the buildings in series before impacting the surrounding moat wall.

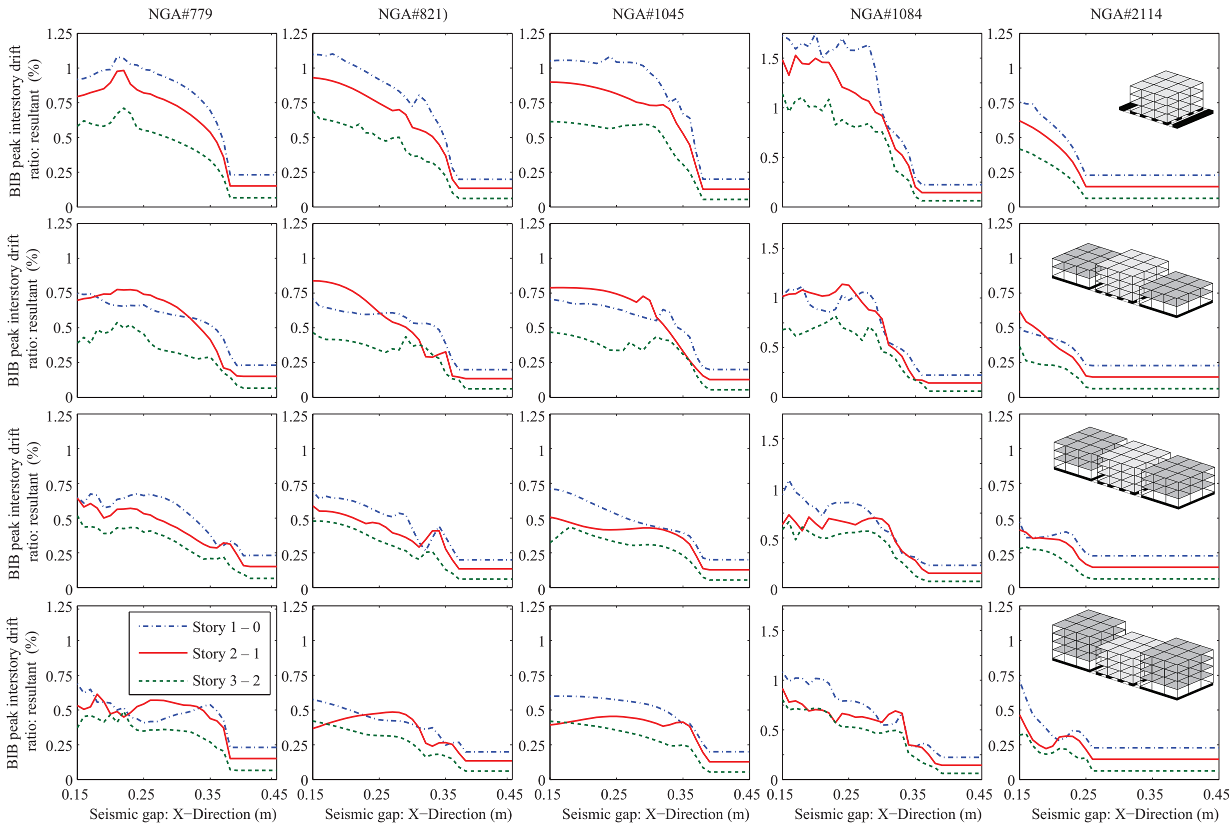

Figure 6: Peak responses at each floor of the 3-story base-isolated building among corner columns in terms of the available gap size for four configurations of the adjacent structures and a fixed angle of incidence set at 0°.

The plots of Figure 7 present the envelopes of the peak interstory deflection ratios, for all six configurations of the base-isolated building (regarding the number of floors and the location of the adjacent fixed-supported buildings) and for the selected bidirectional near-fault ground-motions. The first row of Figure 7 presents the envelopes of the maximum responses considering potential poundings on both sides of the seismically isolated building, while the second row plots the corresponding maximum responses considering only one-sided impacts with the adjacent structure on the east side of the seismically isolated buildings. It is observed that as the separation distance increases the amplifying effects resulting from poundings decrease. Also, the number of stories of the adjacent fixed-supported buildings, and the characteristics of the adjacent structures seem to influence the severity of the impact. Nevertheless, a clear trend cannot be identified. The response of the base-isolated building with adjacent buildings on both sides deviates significantly from the corresponding response in the case of one-sided building for the case of the Northridge earthquake (NGA#1084), while, for all other excitations considered herein, the response is similar. This particular deviation can be attributed to the combined differences in structural arrangement (one side *vs.* both side) and the excitation characteristics. It should be noted that a similar response could be observed for the other seismic excitations presented in Figure 7 if a different incidence angle is considered.

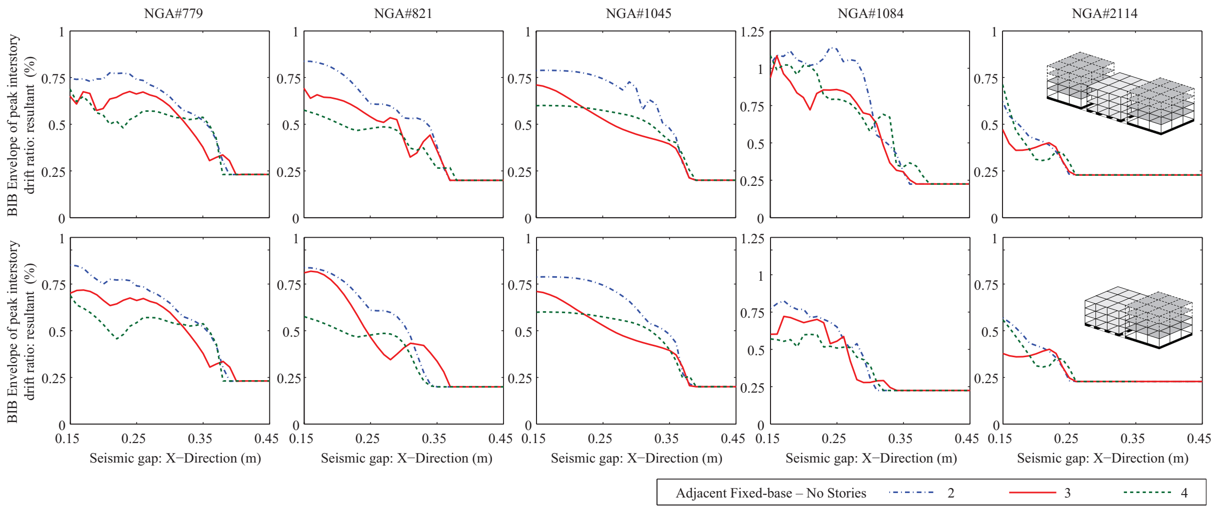

Figure 7: Envelope of peak responses of the base-isolated building among corner columns in terms of the available gap size for different arrangement of the adjacent structures (angle of incidence = 0°).

In order to identify some of the trends that may be observed due to pounding interactions, the response of multiple pairs of buildings (a 3-story base-isolated building and a multi-story fixed-base structure), when subjected to 2 bidirectional excitations of different orientations, are studied. Similar sets of analyses, as those described in the previous subsection, are performed. The structural characteristics of the base-isolated buildings, as well as the isolation characteristics are kept the same. The width of the seismic gap varies with a step of 2.5 cm in the range of 15 cm to 60 cm, while the incidence angle θ varies from 0° to 360° with a step of 15°. The results of those simulations are presented in Figure 8 in terms of polar plots where the envelope of the peak resultant interstory drift ratios is color-coded, whereas the radius of the polar plot represents the magnitude of the seismic gap. The results from more than 3,500 simulations are contained within this figure.

Consistent with previous observations, these contour plots indicate that the direction of the seismic excitation significantly affects the peak interstory drift ratio. It is also observed that pounding is practically eliminated only when the gap is sufficient, with the critical gap size being a function of the earthquake excitation and the structural characteristics. Also, plots in Figure 8 indicate that the characteristics of the adjacent fixed-supported structure seem to play a significant role to the severity of the structural impact. Furthermore, the extent at which the incidence angle influences the peak response depends on the structural systems (e.g. number of stories) and the separation distance. In such circumstances, the term ‘building interaction’ more appropriately describes the overall behavior of the base-isolated building. As expected, the effect of the angle of incidence on the structural response is significantly different due to the location of a fixed-supported building on one side (east).

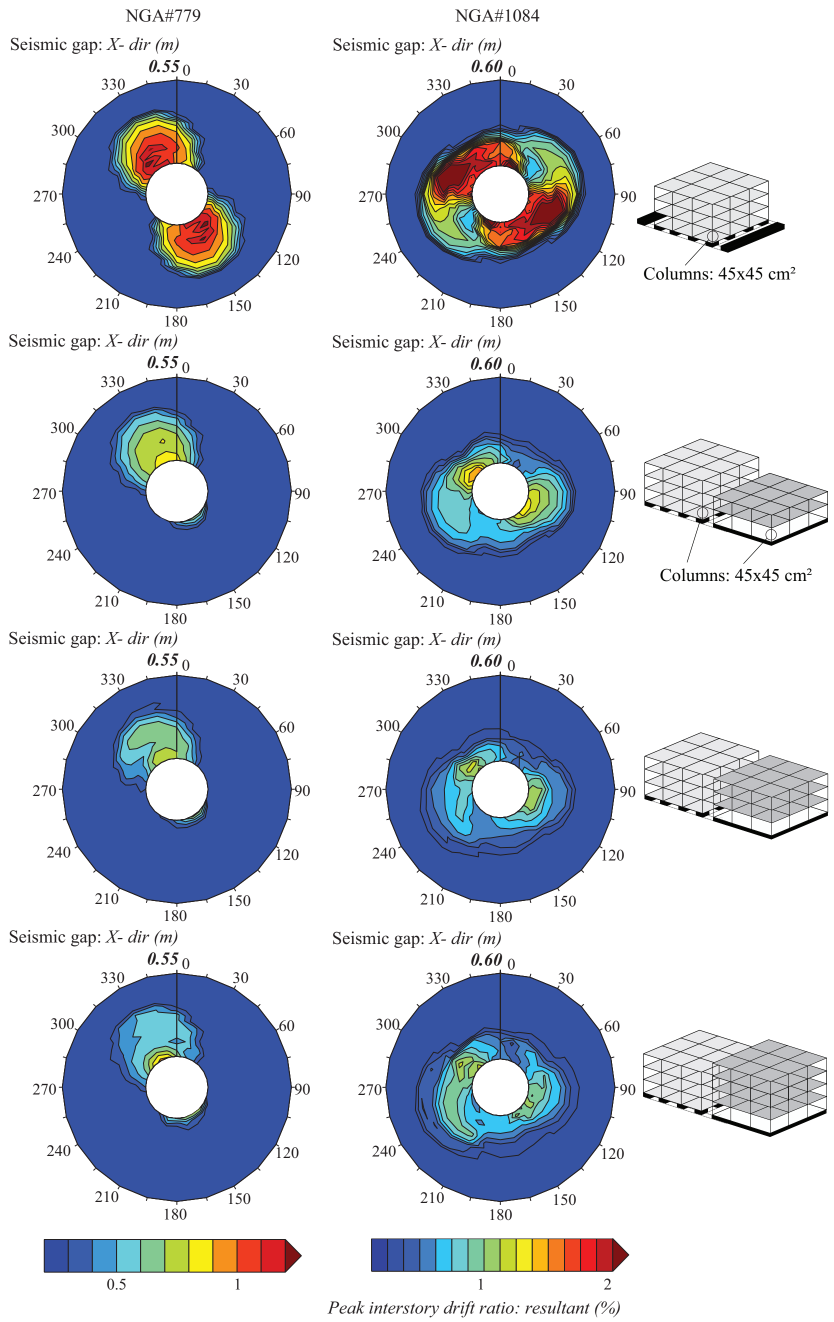

Figure 8: Contour plots of the envelope interstory drifts resultant ratio among corner columns, for various orientations of the ground motions and available gap sizes, and 3 different configurations of the adjacent structures.

4.4 Effect of Adjacent Structures' Characteristics

In the above discussion, the superstructures' flexibilities of both buildings (base-isolated and fixed-based) are assumed to be the same. With the characteristics of the base-isolated structures unchanged, the flexibility of the adjacent buildings is parametrically examined. Different stiffnesses of the superstructure are obtained in this section, by considering different cross-sections of the columns (35 x 35 cm^2). The peak resultant interstory drift ratios are obtained under 2 seismic excitations. Figure 9 presents the effects of the angle of incidence and the gap width on the interstory drift amplification, under the Loma Prieta (1989) and the Northridge (1994) earthquakes.

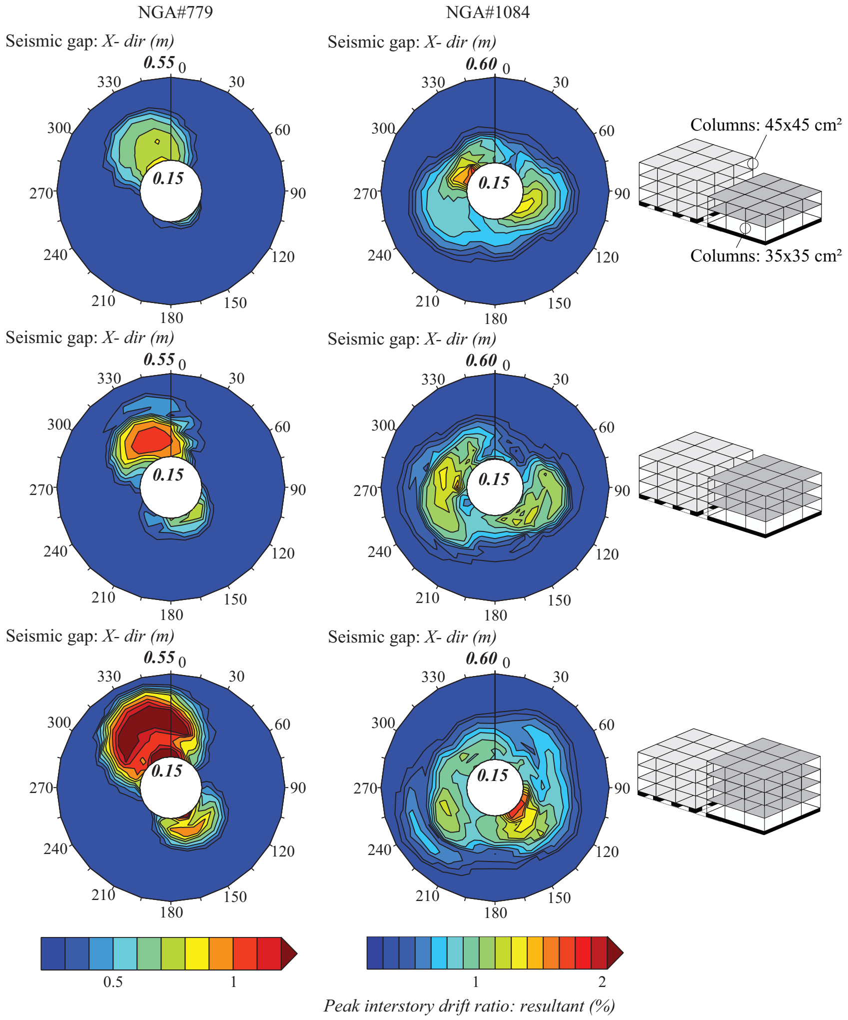

Figure 9: Contour plots of the envelope interstory drift resultant ratio of the 3-story seismically isolated building ratio among corner columns with different characteristics of the adjacent fixed-supported building for various orientations of the ground motions and available gap sizes.

It can be observed that the obtained response, is strongly affected by the orientation of the excitation. The stiffness of the adjacent structures has significant influence on the peak response of the base-isolated structure during impact. Amplified results due to pounding to adjacent 3- and 4-story fixed-supported buildings deviate significantly from the corresponding results presented in Figure 8. The critical gap size required to avoid pounding is, in general, significantly larger especially among critical orientations of the ground motions. Special attention should be given in the case of the Loma Prieta excitation (NGA#779), since the results suggest that when impact to the selected 4-story fixed-based building located at its east side, the base-isolated building's peak resultant interstory drift ratio for incidence angle in the critical range reaches values higher than for the corresponding poundings cases when only moat walls surround the building (relevant results present in Figure 8(a)). This indicates that the interaction between the adjacent structures drives the critical incidence angle, the critical gap size and the severity of the structural pounding.

5 CONCLUSIONS

Parametric studies for simulating earthquake-induced pounding of seismically isolated buildings have been conducted in three-dimensions in order to investigate the influence of the incidence angle, the width of the seismic gap and the flexibility of the superstructure on the peak response of a base-isolated building. Simulation results show that the impacts are particularly unfavourable for the structure since they significantly amplify interstory deflections of the building. Furthermore, they reveal that the detrimental effects of pounding may become more severe for certain values of the excitation angle which, in general, is different from 0 degrees, the most commonly employed direction in practice when performing time-history analysis. The incidence angle, in which the amplification of the superstructure response due to pounding with the adjacent building obtains its maximum value, in case of pounding only to the surrounding moat wall, generally coincides with the angle in which the peak base displacement occurs for the case of pounding to the surrounding wall. On the other hand, one can conclude that the process of determining the critical incidence angle is more complex when considering adjacent multistory structures and since generalizations cannot being made, specific case simulations should be performed on each case for more reliable investigations of the expected peak seismic response.

REFERENCES

1. Matsagar VA, Jangid RS. Seismic response of base-isolated structures during impact with adjacent structures. *Engineering Structures* 2003; **25**(10): 1311–1323. DOI: 10.1016/S0141-0296(03)00081-6.
2. Komodromos P. Simulation of the earthquake-induced pounding of seismically isolated buildings. *Earthquake Engineering and Structural Dynamics* 2008; **86**(7–8): 618–626. DOI: 10.1016/j.compstruc.2007.08.001.
3. Ye K, Li L, Zhu H. A modified Kelvin impact model for pounding simulation of base-isolated building with adjacent structures. *Earthquake Engineering and Engineering Vibration* 2009; **8**(3): 433–446. DOI: 10.1007/s11803-009-8045-4.
4. Dimitrakopoulos E, Makris N, Kappos AJ. Dimensional analysis of the earthquake-induced pounding between adjacent structures. *Earthquake Engineering and Structural Dynamics* 2009; **38**: 867–886. DOI: 10.1002/eqe.872.
5. Mahmoud S, Jankowski R. Pounding-involved response of isolated and non-isolated buildings under earthquake excitation. *Earthquakes and Structures* 2010; **1**(3): 231–252. DOI: 10.12989/eas.2010.1.3.231.
6. Jankowski R, Mahmoud S. *Earthquake-Induced Structural Pounding*. Cham: Springer International Publishing; 2015. DOI: 10.1007/978-3-319-16324-6.
7. Mavronicola E, Polycarpou P, Papaloizou L, Komodromos P. Computer-aided investigation of special issues of the response of seismically isolated buildings. *International Journal of Computational Methods and Experimental Measurements* 2015; **3**(1): 21–32. DOI: 10.2495/CMEM-V3-N1-21-32.
8. Mavronicola EA, Polycarpou PC, Komodromos P. Effect of Planar Impact Modeling on the Pounding Response of Base-Isolated Buildings. *Frontiers in Built Environment* 2016; **2**: 11. DOI: 10.3389/fbuil.2016.00011.
9. Mavronicola E, Polycarpou PC, Komodromos P. The effect of modified linear viscoelastic impact models in the pounding response of a base-isolated building with adjacent structures. *5th International Conference on Computational Methods in Structural Dynamics and Earthquake Engineering*, Crete: 2015.
10. Matsagar VA, Jangid RSS. Impact Response of Torsionally Coupled Base-isolated Structures. *Journal of Vibration and Control* 2010; **16**(11): 1623–1649. DOI: 10.1177/1077546309103271.

11. Jankowski R. Non-linear FEM analysis of earthquake-induced pounding between the main building and the stairway tower of the Olive View Hospital. *Engineering Structures* 2009; **31**(8): 1851–1864. DOI: 10.1016/j.engstruct.2009.03.024.
12. Jankowski R. Non-linear FEM analysis of pounding-involved response of buildings under non-uniform earthquake excitation. *Engineering Structures* 2012; **37**: 99–105. DOI: 10.1016/j.engstruct.2011.12.035.
13. Uz M, Hadi M. Investigating the effects of pounding for inelastic base isolated adjacent buildings under earthquake excitations. In: S. Fragomeni, S. Venkatesan NLSS, editor. *Incorporating Sustainable Practice in Mechanics of Structures and Materials*, 2011.
14. Sato E, Furukawa S, Kakehi A, Nakashima M. Full-scale shaking table test for examination of safety and functionality of base-isolated medical facilities. *Earthquake Engineering and Structural Dynamics* 2011; **40**(13): 1435–1453. DOI: 10.1002/eqe.1097.
15. Pant DR, Wijeyewickrema AC. Structural performance of a base-isolated reinforced concrete building subjected to seismic pounding. *Earthquake Engineering and Structural Dynamics* 2012; **41**(12): 1709–1716. DOI: 10.1002/eqe.2158.
16. Pant DR, Wijeyewickrema AC. Performance of base-isolated reinforced concrete buildings under bidirectional seismic excitation considering pounding with retaining walls including friction effects. *Earthquake Engineering and Structural Dynamics* 2014; **43**(10): 1521–1541. DOI: 10.1002/eqe.2409.
17. Mavronicola E, Polycarpou PC, Komodromos P. Effect of the seismic excitation's incidence angle on the nonlinear behavior of base isolated buildings considering pounding to adjacent moat walls. *VII European Congress on Computational Methods in Applied Sciences and Engineering (ECCOMAS Congress 2016)*, 2016.
18. Mavronicola EA, Polycarpou PC, Komodromos P. Spatial seismic modeling of base-isolated buildings pounding against moat walls: effects of ground motion directionality and mass eccentricity. *Earthquake Engineering & Structural Dynamics* 2016. DOI: 10.1002/eqe.2850.
19. Masroor A, Mosqueda G. Experimental simulation of base-isolated buildings pounding against moat wall and effects on superstructure response. *Earthquake Engineering and Structural Dynamics* 2012; **41**(14): 2093–2109. DOI: 10.1002/eqe.2177.
20. Polycarpou PC, Papaloizou L, Komodromos P. An efficient methodology for simulating earthquake-induced 3D pounding of buildings. *Earthquake Engineering and Structural Dynamics* 2014; **43**(7): 985–1003. DOI: 10.1002/eqe.2383.
21. Wen YK. Method for random vibration of hysteretic systems. *Journal of the Engineering Mechanics Division* 1976; **102**(2): 249–263.
22. Park YJ, Wen YK, Ang A. Random vibration of hysteretic systems under bi-directional ground motions. *Earthquake Engineering and Structural Dynamics* 1986; **14**(4): 543–557. DOI: 10.1002/eqe.4290140405.
23. Nagarajaiah S, Reinhorn AM, Constantinou MC. Nonlinear Dynamic Analysis of 3D Base Isolated Structures. *Journal of Structural Engineering* 1991; **117**(7): 2035–2054. DOI: 10.1061/(ASCE)0733-9445(1991)117:7(2035).